Rational Design of Abasic Site-Containing DNA Triplexes to Bind Small Molecules with Low Nanomolar Dissociation Constants

Jian Liu^a, Tingting Jiang^a, Jiemin Zhao^b, Mingchun Liu^a, Fangfang Chen^a, Lixin Lin^a, Huawei He^c, Hua Zuo^{a*}, Cheng Zhi Huang^{a*}, Chengde Mao^{a,b*}

^a Key Laboratory of Luminescence Analysis and Molecular Sensing (Southwest University), Ministry of Education, College of Pharmaceutical Sciences, Southwest University, Chongqing 400715, China

^b Department of Chemistry, Purdue University, West Lafayette, Indiana 47907, USA
^c State Key Laboratory of Silkworm Genome Biology, Biological Science Research Center,
Southwest University, Chongqing 400715, China

*Corresponding author. Email: zuohua@swu.edu.cn (H. Z.); chengzhi@swu.edu.cn (C. Z. H.); mao@purdue.edu (C. M.).

Abstract

De novo design of functional biomacromolecules is of great interest to a wide range of fundamental science and technological applications, including understanding life evolution and biomacromolecular structures, developing novel catalysts, inventing medicines, and exploring high-performance materials. However, it is an extremely challenging task and its success is very limited. It requires a deep understanding of the relationships among the primary sequences, the 3D structures, and the functions of biomacromolecules. Herein, we report a rational, *de novo* design of a DNA aptamer that can bind melamine with high specificity and high affinity (dissociation constant $K_d = 4.4$ nM). The aptamer is essentially a DNA triplex, but contains an abasic site, to which the melamine binds. The aptamer-ligand recognition involves hydrogen-bonding, π – π stacking, and electrostatic interactions. This strategy has been further tested by designing aptamers to bind to guanosine. It is conceivable that such a rational strategy, with further development, would provide a general framework for designing functional DNA molecules.

Keywords: DNA nanotechnology; DNA aptamer; rational design

Introduction

Being able to rationally design biomacromolecules with specific structures and functions is not only an ultimate test of our understanding of biomacromolecules, ^{1, 2}, but also has wide range of applications in the fields including synthetic biology, medicine, ³ catalysis, ⁴ and advanced materials. ⁵ It is an outstanding challenge. In the recent years, a great progress has been made in protein designs, ^{1, 6-8} though functional demonstrations are much less. ⁴ DNA has also been

extensively explored for construction of nanostructures.⁹⁻¹³ Structural features at the nano-scale can be readily realized.¹⁴⁻¹⁶ To achieve functions (e.g. binding or catalysis), the structural features at the angstrom level are often needed, but realization of such a high-precision is scarce for arbitrarily designed nucleic acids.^{17, 18} Previously, the double stranded DNAs containing abasic site have been reported for the aptamer design of small molecules, riboflavin¹⁹ and theophylline²⁰. A vacancy-bearing DNA scaffolds like duplex, G-quadruplex or other structures acted as an aptamer to bind free purine nucleosides²¹⁻²². Here, we have extended this strategy to abasic site-containing DNA triplexes. To this end, we have *de novo* designed DNA structures (aptamers) that can recognize and bind to specific ligands with high affinities.

EXPERIMENTAL SECTION

Modeling the aptamer structures. Molecular models for Apt^M-MA complex were built by COOT. The complex contained three parts: (i) the T4 loops on both sides, modeled according to a solution NMR structure (pdb: 1A8W); (ii) the triplex, modeled according to a solution NMR structure (pdb: 1D3X) with the sequence mutated to be consistent with the design; (iii) the T-MA-T triplet, modeled from a crystal structure (pdb: 6WK7). All the three pdb files were from Protein Data Bank (https://www.rcsb.org/) and the extra structural parts were removed. The three parts were manually translated and rotated in COOT to be connected with correct distance and DNA polarities. The model was visualized in Pymol with DNA in cartoon or surface mode and the MA in sphere mode.

Assembly of DNA aptamers. The DNA strands were mixed in TAE/Mg²⁺ buffer (40 mM tris base, 20 mM acetic acid, 2 mM EDTA, and 12.5 mM magnesium acetate) with designated pH. The DNA solutions were incubated at 95 °C for 5 min, 65 °C for 30 min, 50 °C for 30 min, 37 °C for 30 min, 25 °C for 30 min and then at 4 °C overnight.

Isothermal Titration Calorimetry. ITC experiment was performed by using MicroCal iTC200 (Malvern Panalytical Ltd.) at 25 °C. For DNA sample preparation, the DNA strands were dissolved in TAE/Mg²⁺ buffer (300 µL) and were incubated at 95 °C for 5 min, 65 °C for 30 min, 50 °C for 30 min, 37 °C for 30 min, 25 °C for 30 min and 4 °C overnight. Before the measurement, the DNA samples were centrifuged for three minutes in a SCILOGEX S1010E centrifuge to remove air bubbles. An aptamer sample in TAE/Mg²⁺ buffer was loaded into a 300 µL ITC cell at 25 °C. Then the corresponding small molecule in the identical buffer was loaded into syringe. Each titration consisted of an initial purge injection of 0.4 µL and either 19 successive injections of 2 μL of ligand or 38 successive injections of 1 μL of ligand (thymine and evanuric acid), with an interval of 120-180 s between injections. For melamine and Apt^M titration at pH 7.0, the injection intervals were 240 s, 600 s, 600 s, 540 s, 540 s, 360 s, 360 s, 240 s, 240 s, and 180 s for the rest 10 injections. After titration, the data was fitted by the Origin 7.0 software licensed by MicroCal and the thermodynamic parameters (N value, Ka, AH and AS) were obtained. The value of the dissociation constant (K_d) was calculated through these thermodynamic parameters. The quality of ITC data was described by the Wiseman coefficient $C = N \cdot [aptamer]/K_d$, where N is the number of binding site. For data with a C value less than 1, we increased the concentration of DNA and small molecules to make the titration reaction saturated. In such case, even if the C value is less than 1, the set of data is still reliable. For each sample, it was repeated at least three times to calculate the average and standard deviation.

Measurement of DNA Melting Temperature (Tm). A solution (pH 5.0) containing 2 uM AptM and 2 uM (or 20 uM, 200 uM) melamine in 1×TAE/Mg²⁺ was heated from 15-95 °C, and the UV absorbance at 260 nm was recorded. 1×TAE/Mg²⁺ buffer (pH 5.0) was used as blank control. The d(Ab)/d(T)-temperature curve was obtained by differentiating and integrating the collected data using Origin software. The absorption-temperature curve was obtained by normalizing the collected data using Origin software.

RESULTS AND DISCUSSION

Rational Design and Characterization of Abasic-Site-Containing DNA Triplex Structure as Binding Scaffold for Melamine. Figure 1 illustrates the strategy to design a DNA aptamer (Apt^M) that can recognize melamine (MA). MA is a flat, aromatic molecule with a threefold rotational symmetry. MA has three identical sides. Each side has a complementary hydrogen (H)-bond pattern with a thymine (T) and can form three H-bonds with a thymine (Fig. 1a).²³ Thus, to bind to an MA, potential interactions could be (i) via lateral H-bonding on the molecular plane with thymine residues (Fig. 1a) and (ii) via vertical π -stacking with other aromatic moieties. To realize these potential interactions, we design the DNA aptamer, Apt^M, based on a DNA triplex structure (Figs. 1b and S1).²⁴⁻²⁷ At the middle of the poly-purine strand, there is a one-base gap. Two thymines are located at the gap-corresponding positions on the two poly-pyrimidine strands. This gap provides a MA-binding pocket. (i) An MA can form six H-bonds with the two thymines. (ii) the MA will interact with the two flanking triplets via π -stacking. To maximize the base stacking, two C-G°C⁺ triplets are used to flank the gap as C-G pairs provide stronger base stacking than A-T pairs. Note that C-G \circ C⁺ triplets form only in acidic environment, e. g. pH = 5.0 (Fig. S2). (iii) The MA will be protonated at pH 5.0. The positively charged MA⁺ remains the capability to form H-bonds with two Ts (Fig. S2d), but provides strong electrostatic interactions with the negatively charged phosphate on the DNA backbones and the partially negatively charged Oatoms on thymines. All the three classes of interactions together will provide a specific and strong association between the MA and the designed DNA aptamer, Apt^M. The geometry of a T-MA-T triplet is very similar to that of a C-G°C⁺ triplet (Fig. 1c).²³ Thus, the T-MA-T triplet can fit into the DNA triplex of the Apt^M to form a continuous triplex structure (Fig.1d). Based on the crystal structures of a poly (T)-MA complex and a DNA triplex, a structural model can be readily built in Coot, a macromolecular model building software.²⁸ Therefore, MA directly binds to the designed binding pocket on Apt^M (Fig. 1e-f).

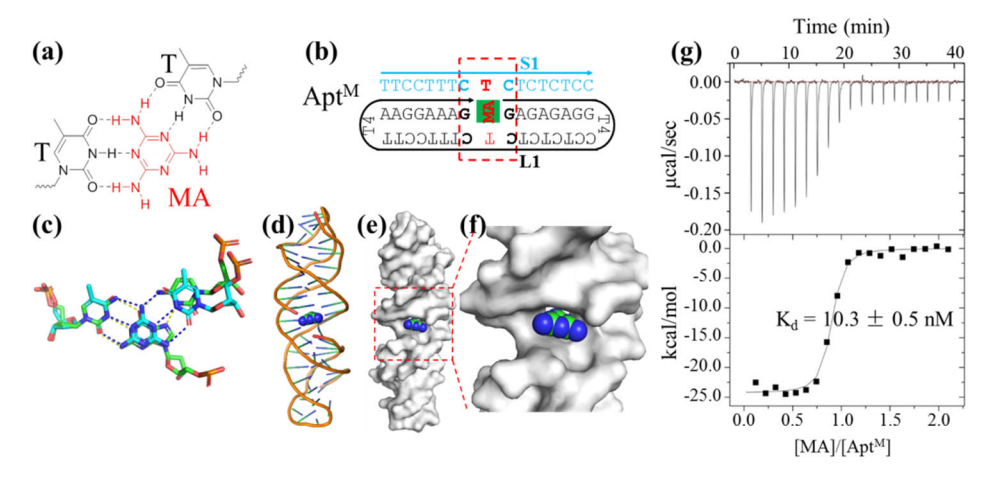


Figure 1. A melamine (MA)-binding DNA aptamer, Apt^M . (a) Structure of a T-MA-T hetero-triplet. (b) Secondary structure Apt^M , consisting of two DNA strands: L1 and S1. The binding pocket and bound MA are highlighted by a red, dash line box and a green rectangle, respectively. (c) Superimposing a T-MA-T triplet (blue) and a C-G $^{\circ}$ C $^{+}$ (green) triplet. (d-f) The molecular model of $Apt^M - MA$. MA shown in sphere mode. (g) An ITC study of MA – Apt^M binding affinity. 3.0 μ M Apt M was titrated with 24 μ M MA.

Table 1. Binding affinity and thermodynamic parameters of aptamer-small molecule binding at 298 K. The values are calculated from at least three independent, repeating measurements.

Aptamer	ligand	рН	n	K _a (x 10 ⁶ M ⁻¹)	K_d	ΔH (kcal/mol)	ΔS (cal/mol/K)
Apt^{M}	MA	5.0	0.9 ± 0.1	97 ± 5	$10 \pm 1 \mathrm{nM}$	-22.9 ± 1.0	-40.2 ± 3.5
	Adenine	5.0	1.3 ± 0.0	34 ± 3	$30 \pm 2 \text{ nM}$	-17.6 ± 2.2	-24.6 ± 7.3
	Thymine	5.0	0.8 ± 0.1	0.02 ± 0.00	$54 \pm 2 \mu M$	-13.6 ± 0.7	-26.1 ± 2.6
	Cytosine	5.0	1.0 ± 0.0	0.0022 ± 0.0001	$465 \pm 18 \mu\text{M}$	-3.3 ± 0.5	4.2 ± 1.7
	GTP	5.0			NA		
	Cyanuric Acid	5.0	0.8 ± 0.2	0.02 ± 0.00	$54 \pm 3 \mu M$	-13.6 ± 1.3	-26.2 ± 4.7
$\mathrm{Apt^{Ma}}$	MA	5.0	1.0 ± 0.0	0.07 ± 0.00	$15 \pm 0 \mu\text{M}$	-13.3 ± 0.6	-22.7 ± 2.2
$\mathrm{Apt}^{\mathrm{Mb}}$	MA	5.0	1.0 ± 0.0	0.0033 ± 0.0002	$304 \pm 16 \mu\text{M}$	-7.6 ± 0.4	-9.3 ± 1.5
Apt ^{Mc}	MA	5.0	0.8 ± 0.1	21 ± 1	$48\pm3~\text{nM}$	-33.4 ± 1.5	-78.9 ± 5.1
Apt^{MA}	MA	5.0	0.7 ± 0.1	232 ± 39	$4.4\pm0.7~\text{nM}$	-30.6 ± 0.2	-64.3 ± 0.9
$\mathrm{Apt}^{\mathrm{MA1}}$	MA	5.0	0.7 ± 0.0	155.0 ± 3.5	$6.5 \pm 0.1 \text{ nM}$	30.6 ± 0.2	-59.6 ± 3.2
$\operatorname{Apt}^{\operatorname{G}}$	Guanosine	5.0	0.9 ± 0.0	4.0 ± 0.2	$249\pm11~\text{nM}$	-23.1 ± 0.9	-47.4 ± 2.9
Apt^{Ga}	Guanosine	5.0	0.9 ± 0.0	13.7 ± 0.7	$73 \pm 4 \mathrm{nM}$	-27.1 ± 0.6	-58.3 ± 2.0
Apt ^{Ga1}	Guanosine	5.0	0.9 ± 0.0	6.9 ± 0.2	$146\pm5~\mathrm{nM}$	-27.0 ± 0.3	-59.2 ± 0.8

NA: The Apt^M – GTP binding is too weak to be detected.

The Apt^M readily assembled from the two component strands L1 and S1 by forming an intermolecular triplex under an acidic condition, pH 5.0, as confirmed by native polyacrylaminde

gel-electrophoresis, nPAGE (Fig. S3). At pH 5.0, S1 and L1 formed a complex and appeared as a sharp band in the gel as a major product with slow mobility (Fig. S3b), confirming the triplex formation. Furthermore, we used isothermal titration calorimetry (ITC) to quantitatively measured the binding affinity of between Apt^M and MA. Apt^M exhibited a high binding affinity, $K_d = 10.3 \pm 0.5$ nM (Fig. 1g, Table 1), at pH 5.0 as expected.

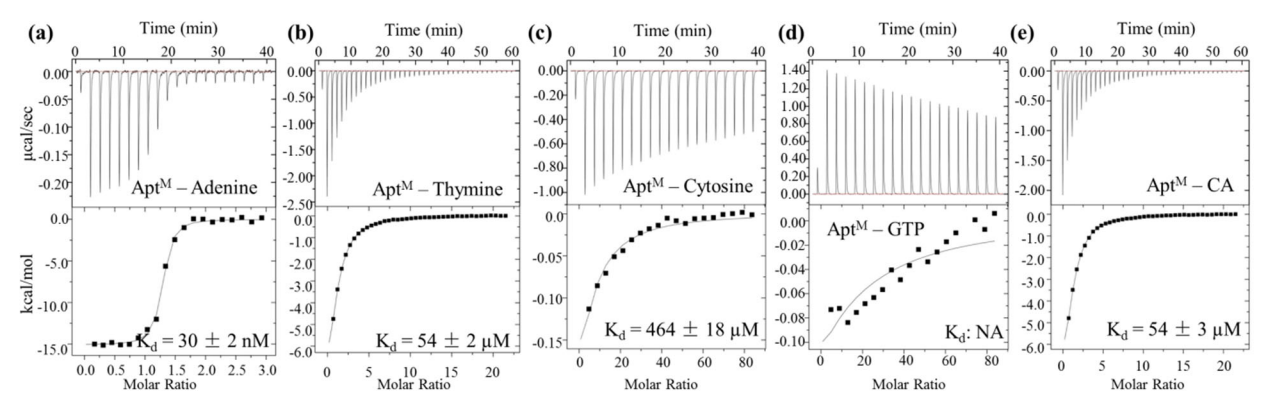


Figure 2. Demonstration of the Apt^M selectivity by ITC study at pH 5.0. Apt^M was titrated with (a) Adenine, (b) Thymine, (c) Cytosine, (d) GTP, (e) Cyanuric acid (CA).

To demonstrate the binding selectivity of Apt^M , we tested the binding between Apt^M and five MA-like molecules: adenine (A), thymine (T), cytosine (C), guanosine triphosphate (GTP) and cyanuric acid (CA) (Figs. 2 and S4; Table 1). For T, C and CA, they bind only poorly to Apt^M and showed very low affinities. The dissociation constant $K_d = 54 \pm 2 \, \mu M$, $465 \pm 18 \, \mu M$, and $54 \pm 3 \, \mu M$ for T, C, and CA, respectively, were over 1000 times higher than the K_d value for MA. GTP doesn't show an appreciable binding to Apt^M even using very high concentrations of Apt^M and GTP. An exception is A. It could form four H-bonds with two-Ts on both sides to form a triplet T-A-T in a similar fashion as T-MA-T triplet; consequently a relative strong $A - Apt^M$ binding (K_d : $30 \pm 2 \, nM$) was observed (Fig. S2). It was still weaker than $MA - Apt^M$ because that there were six H-bonds in a T-MA-T triplet and only four H-bonds in a T-A-T triplet.

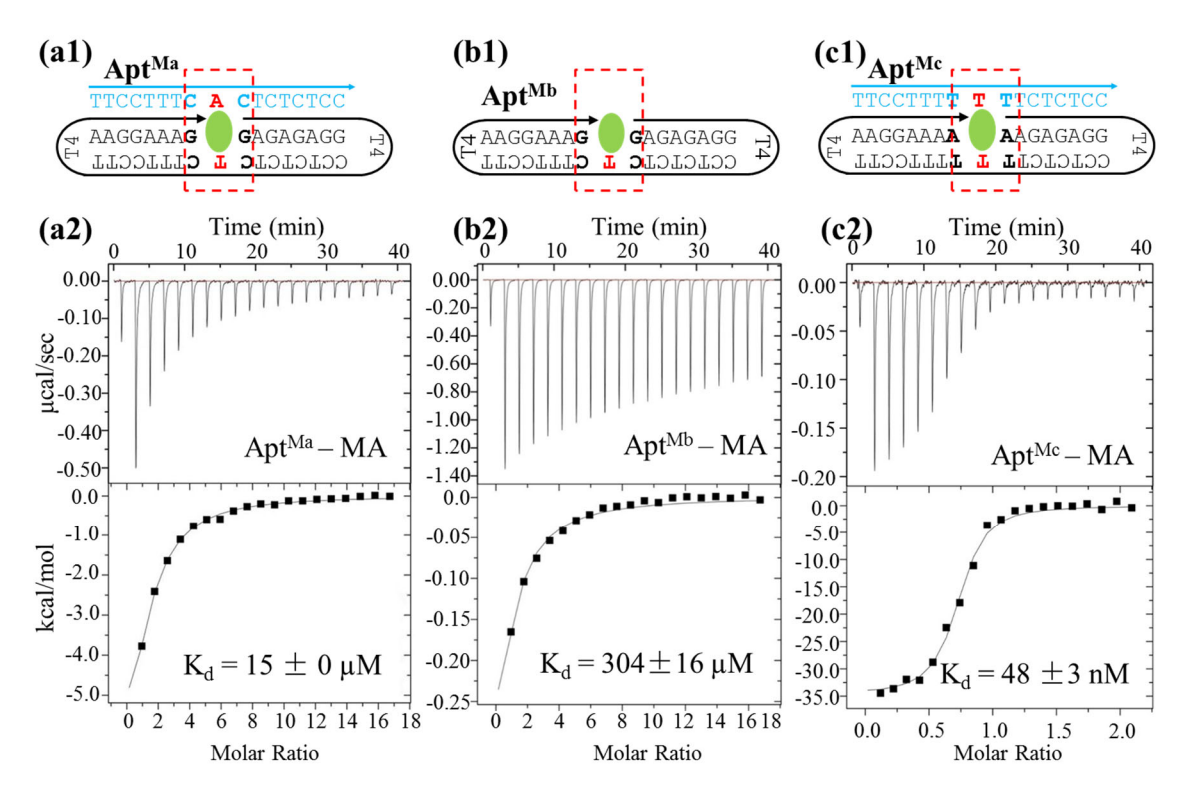


Figure 3. Structural impacts on the aptamer performance studied by ITC at pH 5.0. Top panel: secondary structures of Apt^M mutants (red, dash lined boxes and green ovals indicate the binding pockets and bound ligands, respectively); bottom panel: ITC measurements of the Apt^M mutants and MA binding. (a) Apt^{Ma} examines H-bonding; (b) Apt^{Mb} examines triplex, (c) Apt^{Mc} examines basestacking.

The observed high affinity and selectivity of the designed aptamer Apt^M are attributed to specific H-bonds, base stacking, and electrostatic charge interaction. To confirm the effect of each of these factors, a series of control aptamer mutants (Figs. S1 and S5) are constructed to confirm that those factors contribute to the binding performance of Apt^M (Figure 3). (i) H-bonds. In an aptamer mutant Apt^{Ma} (Fig. 3a), a T in the binding pocket is substituted by an A. An MA can form only three H-bonds with the Apt^{Ma}, instead of six as with Apt^M. No surprise that a much weaker binding ($K_d = 15 \pm 0 \mu M$) is observed for Apt^{Ma}. (ii) Triplex. Another mutant Apt^{Mb} (Fig. 3b) is designed to have the same DNA sequence (Fig. 3b), but lack the triplex-forming oligonucleotide (TFO) S1. Apt^{Mb} will adopt a duplexed structure. In the binding pocket, MA can form only three H-bonds with the Apt^{Mb}. In addition, the gapped duplex is more flexible than a triplex, thus, an even weaker binder would be expected. Indeed, the measured K_d is only $304 \pm 16 \mu M$. Furthermore, since a triplex is not stable at neutral pH, even both strands S1 and L1, even mixed together, could not form a stable Apt^M complex in a neutral buffer (transient formation was possible) as shown in Fig. S3c; consequently, the binding affinity ($K_d = 4.9 \pm 0.9 \mu M$, Table S1) was weak. These two experiments validated that the strong Apt^M-MA binding critically depended on the triplex formation. (iii) Base stacking. In mutant Apt^{Mc} (Fig. 3c), the two flanking C-G°C⁺ triplets are mutated to two T-A°T triplets. Such substitution would decrease the base stacking between the T-MA-T triplet with the flanking triplets, thus, decrease the binding strength. The K_d value is 48 ± 3 nM (Fig. 3c2), slightly worse than that of Apt^M. This series of control experiments have confirmed that all the designed interactions (H-bonding, base stacking, and electrostatic attraction) positively contribute to the strong and specific MA-Apt^M binding (Table 1).

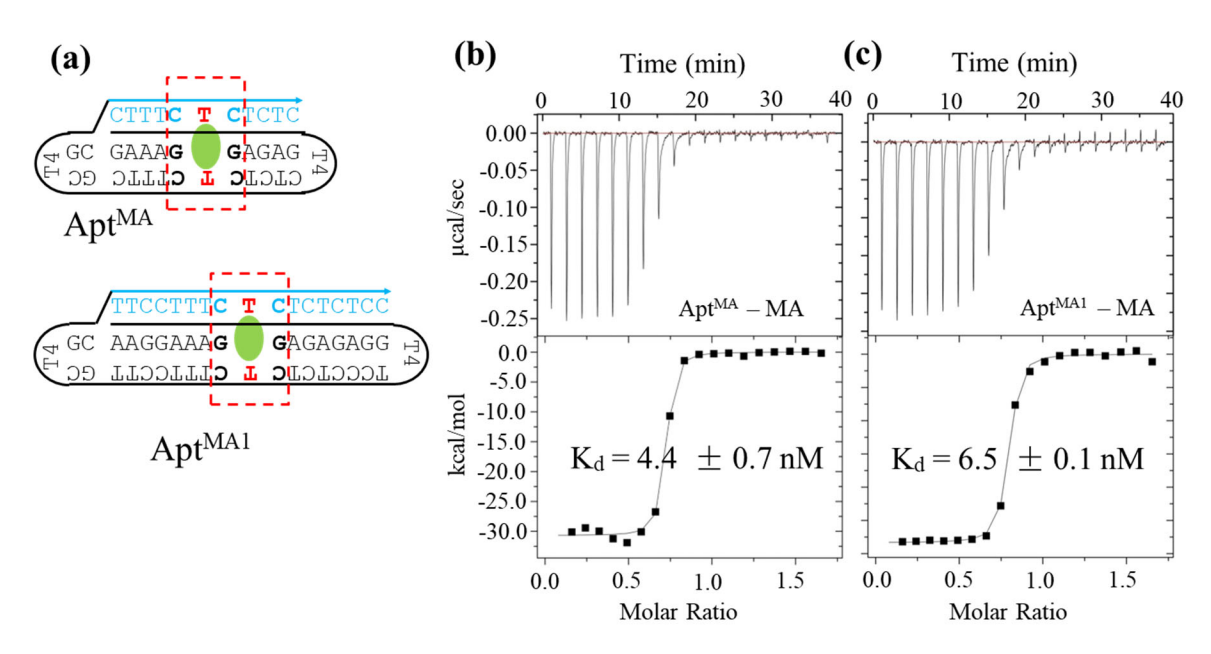


Figure 4. Optimized MA-binding aptamer, Apt^{MA} and Apt^{MA1}. (a) Secondary structure of Apt^{MA} and Apt^{MA1}. (b) and (c) ITC study of MA – Apt^{MA} and MA – Apt^{MA1} binding at pH 5.0.

The Optimization of the Designed Aptamer Apt^M to Apt^{MA} and Apt^{MA1}. The aptamer design can be further optimized (Fig. 4). In Apt^M, the binding pocket involves a gap in the DNA triplex. The triplets immediately flanking the gap are expected to considerably breathe (constantly and transiently break and form), which would weaken the base stacking between T-MA-T triplet and its flanking triplets, leading to additional entropy loss during MA-Apt^M binding. This effect will decrease the ligand-aptamer binding affinity. To partially overcome the breathing effect, we have designed two aptamers, Apt^{MA} and Apt^{MA1}, folded from single DNA strands containing an abasic residue at the place of the gap (Fig. 4a). Apt^{MA} contains 4 bps at each side of the binding pocket, while Apt^{MA1} contains 7 bps. The continuous backbone will likely decrease the breathing effect near the binding approached, thus, increase the binding affinity. Indeed, this design substantially increases the binding affinity and the K_d value changes from 10.3 ± 0.5 nM (for Apt^M) to 4.4 ± 0.7 nM (for Apt^{MA}) (Fig. 4b), and 6.5 ± 0.1 nM (for Apt^{MA1}) (Fig. 4c). We speculate that the length of the triplets at both sides of the binding pocket does not result in significant affinity difference.

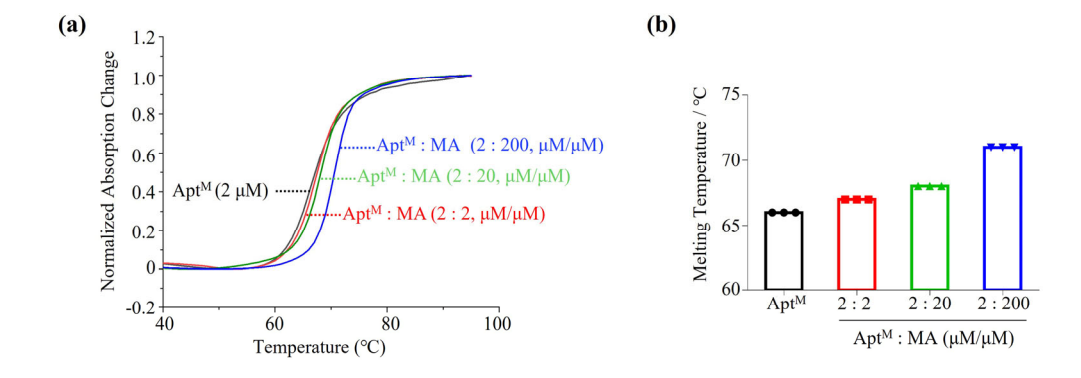


Figure 5. The Tm of Apt^M in the presence of melamine. (a) The normalized UV absorbance of Apt^M and (b) The Tm of Apt^M. 2 μM Apt^M was bound to melamine (0, 2, 20, and 200 μM).

Effects on Thermal Denaturation of Ligand Binding. To further evaluate the effects on thermal denaturation of ligand binding, we analyzed the Tm of Apt^M, which was used for preliminary detection of the melamine sample in solution (Figs. 5 and S6, Table S1). We observed that the differential of UV absorbance and temperature of 2 μ M Apt^M was increased as the concentration of melamine increased (0, 2, 20, and 200 μ M) (Fig. S6a). The ratio of peak height to half-peak width and the ratio of peak height to half-peak width were accordingly increased (Figs. S6b and S6c). In the elevated concentration range of 0-200 μ M melamine, the Tm of Apt^M increased (Fig. 5). We thus suggest Tm would be and effective way for the detection of melamine sample, but further investigations should be carried out.

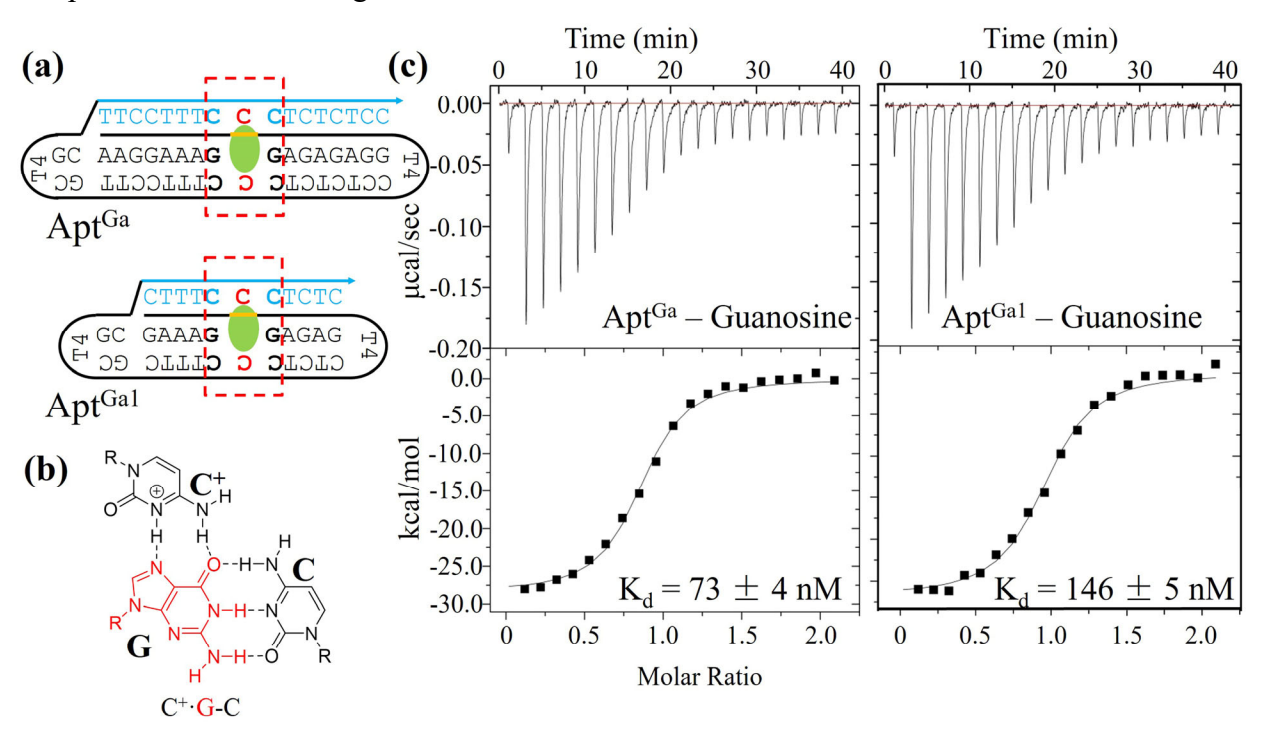


Figure 6. Guanosine-binding DNA aptamers, Apt^{Ga} and Apt^{Ga1}. (a) Secondary structure Apt^G and Apt^{Ga1}, containing an abasic residue at the binding pocket. The binding pocket and bound guanosine are highlighted by a red, dash line box and a green oval, respectively. (b) Structure of a C-G°C⁺ triplet at pH 5.0 at the binding pocket. (c) An ITC study of guanosine – Apt^{Ga1} binding at pH 5.0.

Rational Design and Characterization of Abasic-Site-Containing DNA Triplex Structure as Binding Scaffold for Guanosine. Inspired by the success of MA-binding aptamer Apt^M, we have applied the strategy to design guanosine-binding aptamers, Apt^{Ga} and Apt^{Ga1} (Fig. 6). At pH 5.0, guanosine can form three H-bonds with a cytosine *via* Watson-Crick base pairing and two H-bonds with another protonated cytosine *via* Hoogsteen base pairing as in a C-G°C⁺ triplet, which can fit into a DNA triplex. Accordingly, Apt^{Ga} and Apt^{Ga1} are designed in a similar way to Apt^{MA1} and to Apt^{MA}, respectively, except that the two T bases at the binding pocket are replaced by two C bases. Upon sitting in the binding pocket of Apt^{Ga} and Apt^{Ga1}, guanosine can form five H-bonds with the two Cs laterally and base stacking with the two flanking C-G°C⁺

triplets. These interactions together would provide a specific and strong binding between guanosine and Apt^{Ga} and Apt^{Gal}. ITC measurement confirms that Apt^{Gal} has a high binding affinity to guanosine, $K_d = 73 \pm 4$ nM, and the K_d for guanosine – Apt^{Gal} was 146 ± 5 nM (Fig. 6c and Table 1). The Apt^G could also be designed to be assembled from two DNA strands (Figs. S1 & S7; Table S2) in a similar way as Apt^M. The designed guanosine aptamers also exhibited good selectivity. Thardly binds to Apt^G even at very high concentrations of both T and Apt^G. For A and MA, the K_d at 295 ± 12 μ M, 203 ± 9 μ M, respectively, are around 1000 times higher than the K_d value for guanosine. For C and GTP, they bind to Apt^G with 10- to 20-fold weaker affinity than guanosine.

Interestingly, an MA aptamer was reported from systematic evolution of ligands by exponential enrichment (SELEX).²⁹ There are three main differences between the evolved aptamer and the designed aptamer. (i) The designed Apt^{MA} exhibited more than 100 times higher affinity than the aptamer from SELEX (K_d: 510 nM). (ii) Apt^{MA} has a triplex motif as its binding pocket, but the previous selected aptamer doesn't. (iii) In Apt^{MA}, most of the bases could be mutated as long as the overall triplex structure remains. The most critical bases to the desired molecular recognition are only the two Ts in the binding pocket of Apt^{MA}. The two flanking triplets play a role to a less important extent. This situation is quite different from the SELEX-resulting in aptamer, which often requires a relatively large number of conserved bases in addition to their overall 2D/3D structures. Similarly, the designed Apt^G, Apt^{Ga} and Apt^{Ga1} outperformed the previously reported two guanosine-binding aptamers (which have K_d values of 32 and 780 μM, respectively).^{30, 31}

To recognize adenosine, thymine-rich DNA oligomers were rationally designed and these DNAs and adenosine formed triplex³². Upon interacting with adenosine, adenosine formed N-H-N and N-H-O hydrogen bonds with two thymine molecules in poly(thymine) (poly(T)) DNA and contributed to the Watson-Crick pairing and Hoogsteen pairing. We hypothesized that adenosine may interacted with poly(T) and mediated the assembly of poly(T) into a duplex, where adenosine was wrapped in the formed helices, and thus poly(T) and adenosine formed triplex.

SELEX can potentially generate aptamers for any arbitrary ligand. In contrast, the power of the method reported here is limited now as it heavily relies on our capability to rationally engineer interactions to the ligand and such capability is generally lacking. However, the current, rather simple method might be applied to a large family of compounds that share some structural features as nucleobases in terms of flat aromatic rings and multiple H-bond donors/acceptors. In the fundamental DNA science, this study prompts us to ask: why has SELEX not generated DNA structures similar to the designed aptamers? We speculate that the current SELEX protocol has some intrinsic limitations that do not apply to the rational design approach. (i) In addition to the limit of sequence space, the tested buffer conditions are often limited. For example, most of the selection is conducted in neutral solution (generally preferred because it is near the physiological pH). Indeed, it is hardly seen that any DNA triplex structure was in the aptamers discovered from SELEX because C-G°C⁺ triplet is only stable at acidic solution (e.g. pH 5.0). Though such experimental conditions could be easily changed, it is not practical to test a huge number of random solution conditions for not exponentially increasing the workload. (ii) The construct of the DNA library needs conserved sequences at both ends to serve as PCR primer-binding sites for DNA amplification. Such sequences are not subject to selection. Consequently, both ends of a DNA strand are unlikely to play important roles for aptamer-ligand binding. In the designed aptamers reported here, the two free ends are critical for producing the ligand-binding pockets. (iii) As

efficient PCR amplification is critical for SELEX, strong secondary structures will be excluded in SELEX. Thus, aptamers from SELEX are unlikely to have very strong secondary structures.

CONCLUSIONS

In summary, we have developed a strategy to rationally design high-performance DNA aptamers based on abasic site-containing DNA triplexes to recognize nucleobase-like molecules. It will benefit aptamer-based molecular devices, improving their diagnostic and therapeutic efficacy. Such design, along with other related works, 33-35 is not only a test on our current understanding/knowledge of the basic principles that determine DNA structures, but also, we hope, will stimulate exploration of rational designing functional DNA molecules in general and provide insights to improve the widely used SELEX method. 36, 37

Supporting Information. The materials, experimental methods, and the figures and tables to show the DNA-small molecules interactions are supplied as Supporting Information.

Acknowledgements This work was supported by NSFC (22134005, 21974111 and 22274135), NSF (CCF-2107393 to C. M.), and Chongqing Research Program of Basic Research and Frontier Technology, China (cstc2021jcyj-msxmX0931, cstc2021jcyj-msxmX1033 and cstc2020jcyjmsxmX0947). We would like to thank Prof Drs. Jianxiang Zhang, Xun Gou (College of Life Science, Sichuan Normal University), Han Kang (Center of Growth, Metablism and Aging, Sichuan University), and Yongping Shao (Frontier Institute of Science and Technology, Xi'an Jiaotong University) for the assistance with Isothermal Titration Calorimetry analysis (MicroCal iTC200, GE Healthcare).

References

- Cao, L.; Coventry, B.; Goreshnik, I.; Huang, B.; Sheffler, W.; Park, J. S.; Jude, K. M.; Markovic, I.; Kadam, R. U.; Verschueren, K. H. G.; Verstraete, K.; Walsh, S. T. R.; Bennett, N.; Phal, A.; Yang, A.; Kozodoy, L.; DeWitt, M.; Picton, L.; Miller, L.; Strauch, E. M.; DeBouver, N. D.; Pires, A.; Bera, A. K.; Halabiya, S.; Hammerson, B.; Yang, W.; Bernard, S.; Stewart, L.; Wilson, I. A.; Ruohola-Baker, H.; Schlessinger, J.; Lee, S.; Savvides, S. N.; Garcia, K. C.; Baker, D. Design of Protein-Binding Proteins from the Target Structure Alone. *Nature* 2022, 605, 551–560. DOI: 10.1038/s41586-022-04654-9
- 2. Chalkley, M. J.; Mann, S. I.; Degrado, W. F. *De novo* Metalloprotein Design. *Nat. Rev. Chem* 2022, 6, 31–50. DOI:10.1038/s41570-021-00339-5
- 3. Boyoglu-Barnum, S.; Ellis, D.; Gillespie, R. A.; Hutchinson, G. B.; Park, Y.; Moin, S. M.; Acton, O. J.; Ravichandran, R.; Murphy, M.; Pettie, D.; Matheson, N.; Carter, L.; Creanga, A.; Watson, M. J.; Kephart, S.; Ataca, S.; Vaile, J. R.; Ueda, G.; Crank, M. C.; Stewart, L.; Lee, K. K.; Guttman, M.; Baker, D.; Mascola, J. R.; Veesler, D.; Graham, B. S.; King, N. P.; Kanekiyo, M. Quadrivalent Influenza Nanoparticle Vaccines Induce Broad Protection. *Nature* 2021, 592, 623–628. DOI: 10.1038/s41586-021-03365-x

- 4. Hosseinzadeh, P.; Marshall, N. M.; Chacón, K. N.; Yu, Y.; Nilges, M. J.; New, S. Y.; Tashkov, S. A.; Blackburn, N. J.; Lu, Y. Design of a Single Protein That Spans the Entire 2-V Range of Physiological Redox Potentials. *Proc. Natl. Acad. Sci. U.S.A.* 2015, 113, 262–267. DOI: 10.1073/pnas.1515897112
- 5. Choi, T. S.; Tezcan, F. A. Overcoming Universal Restrictions on Metal Selectivity by Protein Design. *Nature* 2022, 603, 522–527. DOI: 10.1038/s41586-022-04469-8
- 6. Zhou, J.; Panaitiu, A. E.; Grigoryan, G. A General-Purpose Protein Design Framework Based on Mining Sequence–Structure Relationships in Known Protein Structures. *Proc. Natl. Acad. Sci. U.S.A.* 2019, 117, 1059–1068. DOI: 10.1101/431635
- 7. Pan, X.; Kortemme, T. Recent Advances in *de novo* Protein Design: Principles, Methods, and Applications. *J. Biol. Chem.* 2021, 296, 100558. DOI: 10.1016/j.jbc.2021.100558
- 8. Kuhlman, B.; Bradley, P. Advances in Protein Structure Prediction and Design. *Nat. Rev. Mol. Cell Biol.* 2019, 20, 681–697. DOI: 10.1038/s41580-019-0163-x
- 9. Seeman, N. C. DNA Nanotechnology at 40. *Nano Lett.* 2020, 20, 1477–1478. DOI: 10.1021/acs.nanolett.0c00325
- 10. Aldaye, F. A.; Palmer, A. L.; Sleiman, H. F. Assembling Materials with DNA as the Guide. *Science* 2008, 321, 1795–1799. DOI: 10.1126/science.1154533
- 11. Jones, M. R.; Seeman, N. C.; Mirkin, C. A. Programmable Materials and the Nature of the DNA Bond. *Science* 2015, 347, 1260901. DOI: 10.1126/science.1260901
- 12. Raezani, H.; Dietz, H. Building Machines with DNA Molecules. *Nat. Rev. Genet.* 2020, 21, 5–26. DOI: 10.1038/s41576-019-0175-6
- 13. Don, J.; Zhou, C.; Wang, Q. Towards Active Self-Assembly through DNA Nanotechnology. *Top. Curr. Chem.* **33**, 1–25 (2020). DOI: 10.1007/s41061-020-0297-5
- 14. Ge, Z.; Fu, H.; Li, Q.; Fan, C. Concept and Development of Framework Nucleic Acids. *J. Am. Chem. Soc.* 2018, 140, 17808–17819. DOI: 10.1021/jacs.8b10529
- 15. Zhang, F.; Nangreave, J.; Liu, Y.; Yan, H. Structural DNA Nanotechnology: State of the Art and Future Perspective. *J. Am. Chem. Soc.* 2014, 136, 11198–11211. DOI: 10.1021/ja505101a
- 16. Pinheiro, A. V.; Han, D.; Shih, W. M.; Yan, H. Challenges and Opportunities for Structural DNA Nanotechnology. *Nat. Nanotechnol.* 2011, 6, 763–772. DOI: 10.1038/nnano.2011.187
- 17. Martin, T. G.; Bharat, T. A. M.; Joerger, A. C.; Bai, X.; Praetorius, F.; Fersht, A. R.; Dietz, H.; Scheres, S. H. W. Design of a Molecular Support for Cryo-EM Structure Determination. *Proc. Natl. Acad. Sci. U.S.A.* 2016, 113, E7456–E7463. DOI: 10.1073/pnas.1612720113
- 18. Wengel, J. Nucleic Acid Nanotechnology Towards Ångström-Scale Engineering. *Org. Biomol. Chem.* 2004, 2, 277–280. DOI: 10.1039/b313986g
- 19. Sankaran, N. B.; Nishizawa, S.; Seino, T.; Yoshimoto K.; Teramae, N. Abasic-Site-Containing Oligodeoxynucleotides as Aptamers for Riboflavin. *Angew. Chem. Int. Ed.* 2006, 45, 1563 1568. DOI: 10.1002/ange.200502979

- 20. Li, M.; Sato, Y.; Nishizawa, S.; Seino, T.; Nakamura, K.; Teramae, N. 2-Aminopurine-Modified Abasic-Site-Containing Duplex DNA for Highly Selective Detection of Theophylline. *J. Am. Chem. Soc.* 2009, 131, 2448–2449. DOI: 10.1021/ja8095625
- 21. Li, X.; Zheng, K.; Zhang, J.; Liu, H.; He, Y.; Yuan, B.; Hao, Y.; Tan, Z. Guanine-Vacancy–Bearing G-Quadruplexes Responsive to Guanine Derivatives. *Proc. Natl. Acad. Sci. U.S.A.* 2015, 112, 14581–14586. DOI: 10.1073/pnas.1516925112
- 22. Li, Y.; Liu, J. Highly Specific Recognition of Guanosine Using Engineered Base-Excised Aptamers. *Chem. Eur. J.* 2020, 26, 13644–13651. DOI: 10.1002/chem.202001835
- 23. Li, Q.; Zhao, J.; Liu, L.; Jonchhe, S.; Rizzuto, F. J.; Mandal, S.; He, H.; Wei, S.; Sleiman, H. F.; Mao, H.; Mao, C. A Poly(thymine) Melamine Duplex for the Assembly of DNA Nanomaterials. *Nat. Mater.* 2020, 19, 1012–1018. DOI: 10.1038/s41563-020-0728-2
- 24. Jain, A.; Wang, G.; Vasquez, K. M. DNA Triple Helices: Biological Consequences and Therapeutic Potential. *Biochimie* 2008, 90, 1117–1130. DOI: 10.1016/j.biochi.2008.02.011
- 25. Vasquez, K. M.; Glazer, P. M. Triplex-Forming Oligonucleotides: Principles and Applications. *Q. Rev. Biophys.* 2002, 35, 89–107. DOI: 10.1017/s0033583502003773
- 26. Amodio, A.; Zhao, B.; Porchetta, A.; Idili, A.; Castronovo, M.; Fan, C.; Ricci, F. Rational Design of pH-Controlled DNA Strand Displacement. *J. Am. Chem. Soc.* 2014, 136, 16469–16472. DOI: 10.1021/ja508213d
- 27. Rusling, D. A.; Chandrasekaran, A. R.; Ohayon, Y. P.; Brown, T.; Fox, K. R.; Sha, R.; Mao, C.; Seeman, N. C. Functionalizing Designer DNA Crystals with a Triple-Helical Veneer. *Angew. Chem. Int. Ed.* 2014, 53, 3979–3982. DOI: 10.1002/ange.201309914
- 28. Emsley, P.; Cowtan K. Coot: Model-Building Tools for Molecular Graphics. *Acta Crystallogr., Sect. D: Struct. Biol.* 2004, 60, 2126–2132. DOI: 10.1107/S0907444904019158
- 29. Gu, C.; Lan, T.; Shi, H.; Lu, Y. Portable Detection of Melamine in Milk Using a Personal Glucose Meter Based on an *in vitro* Selected Structure-Switching Aptamer. *Anal. Chem.* 2015, 87, 7676–7682. DOI: 10.1021/acs.analchem.5b01085
- 30. Connell, G. J.; Yarus, M. RNAs with Dual Specificity and Dual RNAs with Similar Specificity. *Science* 1994, 264, 1137–1141. DOI: 10.1126/science.7513905
- 31. Li, Y.; Liu, J. Highly Specific Recognition of Guanosine Using Engineered Base-Excised Aptamers. *Chem. Eur. J.* 2020, 26, 13644–13651. DOI: 10.1002/chem.202001835
- 32. Liu, M.; Chen, H.; Huang, Y.; Liu, J.; Chen, Q.; Zuo, H.; Fang, L. Mao, C. Enriching Adenosine by Thymine-Rich DNA Oligomers. *Analyst* 2023, 148, 1858–1866. DOI: 10.1039/d3na00297g
- 33. Wang, Y.; Sun, Q.; Zhu, L.; Zhang, J.; Wang, F.; Lu, L.; Yu, H.; Xu, Z. Zhang, W. Triplex Molecular Beacons for Sensitive Recognition of Melamine Based on Abasic-Site-Containing DNA and Fluorescent Silver Nanoclusters. *Chem. Commun.* 2015, 51, 7958–7961. DOI: 10.1039/c5cc01660f
- 34. Zhuang, Z.; Pan, R.; Zhang, Q.; Huang, H. Molecular Recognition of Pyrimidine Nucleobases by Triplex DNA Receptors. *Bioorg. Med. Chem. Lett.* 2015, 25, 1520–1524. DOI: 10.1016/j.bmcl.2015.02.019

- 35. Feldner, T.; Wolfrum, M.; Richert, C. Turning DNA Binding Motifs into a Material for Flow Cells. *Chem. Eur. J.* 2019, 25, 15288–15294. DOI: 10.1002/chem.201903631
- 36. Wilson, D. S.; Szostak, J. W. *In vitro* Selection of Functional Nucleic Acids. *Annu. Rev. Biochem.* 1999, 68, 611–647. DOI: 10.1146/annurev.biochem.68.1.611
- 37. Komarova, N.; Kuznetsov, A. Inside the Black Box: What Makes SELEX Better? *Molecules*. 2019, 24, 3598. DOI: 10.3390/molecules24193598

For Table of Contents Only

